

PARAMETER ESTIMATION IN ULTRASONIC MEASUREMENTS ON TRABECULAR BONE

Karen R. Marutyan, PhD^{*}, Christian C. Anderson, MA[†], Keith A. Wear
PhD^{**}, Mark R. Holland, PhD[†], James G. Miller, PhD[†] and G. Larry
Bretthorst, PhD^{*}

^{}Biomedical Magnetic Resonance Laboratory, Mallinckrodt Institute of Radiology, Washington
University, St. Louis, MO 63110*

[†]Laboratory For Ultrasonics, Department of Physics, Washington University, St. Louis, MO 63130

*^{**}U.S. Food and Drug Administration, Center for Devices and Radiological Health, Silver Spring,
MD 20993, USA*

Abstract. Ultrasonic tissue characterization has shown promise for clinical diagnosis of diseased bone (e.g., osteoporosis) by establishing correlations between bone ultrasonic characteristics and the state of disease. Porous (trabecular) bone supports propagation of two compressional modes, a fast wave and a slow wave, each of which is characterized by an approximately linear-with-frequency attenuation coefficient and monotonically increasing with frequency phase velocity. Only a single wave, however, is generally apparent in the received signals. The ultrasonic parameters that govern propagation of this single wave appear to be causally inconsistent [1]. Specifically, the attenuation coefficient rises approximately linearly with frequency, but the phase velocity exhibits a *decrease* with frequency. These inconsistent results are obtained when the data are analyzed under the assumption that the received signal is composed of one wave. The inconsistency disappears if the data are analyzed under the assumption that the signal is composed of superposed fast and slow waves. In the current investigation, Bayesian probability theory is applied to estimate the ultrasonic characteristics underlying the propagation of the fast and slow wave from computer simulations. Our motivation is the assumption that identifying the intrinsic material properties of bone will provide more reliable estimates of bone quality and fracture risk than the apparent properties derived by analyzing the data using a one-mode model.

INTRODUCTION

Osteoporosis is a disease that results in a decrease in the mineral density of trabecular bone, a porous material that fills the inner cavity of bones. By establishing correlations between ultrasonic parameters and mineral density of trabecular bone, ultrasonic tissue characterization has become an accepted method for clinical diagnosis of osteoporosis [2, 3]. The physics of ultrasound interaction with the composite structure of bone is not yet completely understood. In most measurements a single wave is apparent in the acquired signals [1, 3]. However, the propagation of two types of compressional waves, known as a fast and a slow wave, has been independently observed by several researches [1, 2, 4]. Furthermore, the ultrasonic characteristics of bone appear to violate the conditions imposed by causality. In particular, as illustrated in Fig. 1, for media with an attenuation coefficient that rises approximately linearly with frequency, such as

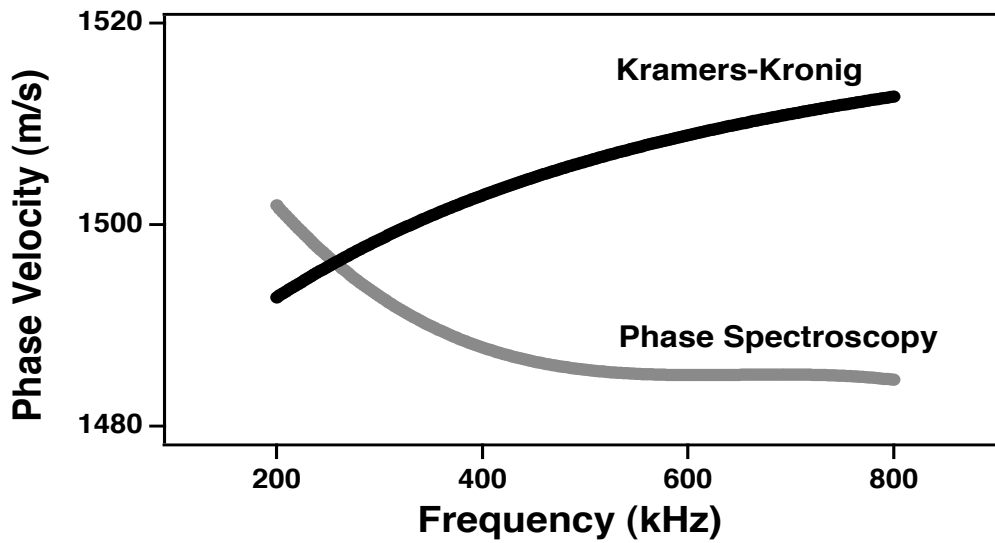


FIGURE 1. This figure illustrates the apparent inconsistency in the ultrasound measurements on bone. The phase velocity inferred from phase spectroscopy analysis exhibits negative dispersion. However, the phase velocity predicted from the attenuation coefficient using the nearly-local approximation of the Kramers-Kronig relations (Eq. 5) rises logarithmically with frequency

bone, the nearly-local approximation of the Kramers-Kronig relations [1] suggests that an increase of phase velocity with frequency or *positive* dispersion should be expected, as opposed to the decrease with frequency or *negative* dispersion that is often reported. These inconsistent results are obtained when the data are analyzed under the assumption that the received signal is composed of one wave. However, this inconsistency disappears if the data are analyzed under the assumption that the signal is composed of superposed fast and slow waves [5].

The motivation for the current study is the assumption that identifying the true ultrasonic properties of bone will provide a more reliable estimate of bone quality and fracture risk than the apparent properties derived from conventional techniques. Consequently, our objective is to make the best possible inferences about the ultrasonic characteristics of bone given that the data consist of two interfering fast and slow waves [1, 2]. Bayesian probability theory provides a powerful and well-developed apparatus tailored to solving problems of this kind. In what follows, we will first review the model for ultrasonic propagation in trabecular bone, apply Bayesian probability theory to compute the posterior probability for each parameter in the model. Finally, we apply the calculations to simulation data to determine how accurately the parameters for two interfering modes can be estimated.

MODEL FOR ULTRASONIC PROPAGATION

For linear ultrasound propagation, the real-valued time-series data are related to the complex spectrum of the propagated pulse via the discrete Fourier transform:

$$d_i = \text{Real} \left[\frac{1}{N} \sum_{j=1}^N P_j \exp\{-i\omega_j t_i/N\} \right] + n_i \quad (1)$$

where d_i is a data value sampled at time t_i , P_j is a value of the complex spectrum at angular frequency ω_j , N is a number of points in the data, and as n_i is a real additive noise.

The data are modeled as the sum of the fast and slow modes. In the frequency domain this sum is given by

$$P_j = \gamma A_j H_{fast,j} + (1 - \gamma) A_j H_{slow,j} \quad (2)$$

where A_j is the complex spectrum of ultrasonic pulse prior to propagation through the bone. The fractional amplitude γ expresses what fraction of the signal amplitude is in the fast wave. Quantitatively γ varies from 0 (only a slow wave propagates) to 1 (only a fast wave propagates). The quantities $H_{fast,j}$ and $H_{slow,j}$ characterize the material properties of medium and are commonly called as the medium transfer functions. The transfer functions govern the ultrasonic propagation of the fast and slow waves and have identical functional form for each mode. Therefore, only the equations for the fast mode are given below. Equivalent formulas for the slow mode are realized on the replacement of the label *fast* by *slow*.

For linear plane wave propagation $H_{fast,j}$ is given as

$$H_{fast,j} = \exp\{-\alpha_{fast,j} l\} \exp\{-i\omega_j l/v_{fast,j}\} \quad (3)$$

in which l is the specimen thickness, $v_{fast,j}$ is the phase velocity and $\alpha_{fast,j}$ is the (linear-with-frequency) attenuation coefficient:

$$\alpha_{fast,j} = \beta_{fast} \frac{\omega_j}{2\pi}. \quad (4)$$

The parameter β_{fast} is frequently referred to as the slope of attenuation.

The slope of attenuation, and therefore the attenuation coefficient, and phase velocity of the medium are not independent. The interrelation between these properties mathematically are expressed through the nearly-local approximation of the Kramers-Kronig relations [1]. For media characterized with an approximately linear-with-frequency attenuation coefficient, such as bone, the nearly-local approximation takes the form

$$v_{fast,j} \approx v_{fast} + \frac{\beta_{fast}}{\pi^2} v_{fast}^2 \ln\left(\frac{\omega_j}{\omega_r}\right) \quad (5)$$

in which v_{fast} is a phase velocity at some arbitrarily chosen reference angular frequency ω_r . Following the earlier study [5] the reference frequency $\omega_r/2\pi$ of 300kHz is used in the calculations presented here.

BAYESIAN CALCULATIONS

The objective is to evaluate the posterior probability density functions for each parameter appearing in the model. These probability densities can be computed from the joint posterior probability for all of the parameters. Consequently, in what follows we will compute the joint posterior probability for all the parameters and then use a Markov chain Monte Carlo simulation with simulated annealing to approximate the respective posterior density functions.

If we denote $\Theta \equiv \{\beta_{fast}, \beta_{slow}, v_{fast}, v_{slow}, \gamma\}$, then joint posterior probability for Θ given all the data D and background information I , $P(\Theta|DI)$, is given by the Bayes' theorem

$$P(\Theta|DI) = \frac{P(\Theta|I)P(D|\Theta I)}{P(D|I)} \quad (6)$$

where the prior probability for the data $P(D|I)$ is a normalization constant and may be dropped provided we normalize this density functions at the end of the calculation, $P(\Theta|I)$ is the joint prior probability for the parameters, and $P(D|\Theta I)$ is the direct probability for the parameters.

Assuming that the parameters are logically independent, the joint prior probability can be factored using the product rule

$$P(\Theta|I) = P(v_{slow}|I)P(v_{fast}|I)P(\beta_{slow}|I)P(\beta_{fast}|I)P(\gamma|I) \quad (7)$$

where we have one prior for each parameter appearing in the model. Each prior probability in Eq. (7) is assigned using a bounded Gaussian to represent what is known about each of the parameters. Specifically, the prior probability for k th parameter in Θ is given by

$$P(\Theta_k|I) \propto \begin{cases} \exp\left\{-\frac{[\Theta_k - M_k]^2}{2\delta_k^2}\right\} & \text{if } L_k \leq \Theta_k \leq H_k \\ 0 & \text{otherwise} \end{cases} \quad (8)$$

where M_k , δ_k , L_k and H_k are the mean, standard deviation and the low and high bounds for the respective parameters. The quantities M_k , δ_k , L_k and H_k are assumed known.

The direct probability for data given Θ , $P(D|\Theta I)$, cannot yet be assigned because it is a marginal probability. To assign this direct probability, the standard deviation of the noise prior probability must be introduced into the calculation. Applying the sum and product rules gives

$$P(D|\Theta I) = \int P(D|\Theta \sigma I)P(\sigma|I)d\sigma \quad (9)$$

where $P(\sigma|I)$ is the prior probability for the standard deviation of the noise prior and $P(D|\Theta \sigma I)$ is the direct probability for the data given both Θ and σ or, in this case, the likelihood. The prior probability for σ is typically assigned using a Jeffreys' prior [6]

$$P(\sigma|I) \propto \frac{1}{\sigma}. \quad (10)$$

The direct probability for the data given both Θ and σ will be assigned using a Gaussian noise prior probability

$$P(D|\Theta\sigma I) = (2\pi\sigma^2)^{-N/2} \exp\left\{-\frac{Q}{2\sigma^2}\right\} \quad (11)$$

where Q is the sum of squared difference between data and the model

$$Q = \sum_{i=1}^N \left(d_i - \text{Real} \left[\frac{1}{N} \sum_{j=1}^N P_j \exp\{-i\omega_j t_i / N\} \right] \right)^2. \quad (12)$$

Substituting Eq. (10) and (11) into Eq. (9) and performing integration over σ yields

$$P(D|\Theta I) \propto Q^{-\frac{N}{2}} \quad (13)$$

which is of the form of Student's t -distribution.

This completes the assignment of the joint posterior probability for the parameters, $P(\Theta|DI)$. The program that implements this calculation uses a Markov chain Monte Carlo simulation with simulated annealing to draw samples from this joint posterior probability density function. At the end of the annealing phase samples are drawn from this joint posterior probability and Monte Carlo integration is then used to obtain samples from the marginal posterior probability for each parameter.

DISCUSSION

There is increasing evidence that ultrasonic signals acquired on bone are comprised of the overlapping fast and slow waves [2, 3, 5]. Because the conventional broadband spectroscopy analyses assume a single mode in the data, there is a need for an alternative analysis appropriate for the multi-modal signals.

In the current study the feasibility for accurate estimation of the bone parameters is investigated by applying Bayesian probability theory to the simulated bimodal data. The parameters used to generate this data were assigned from the empirical values as: $\beta_{fast} = 20\text{dB/cm/MHz}$, $\beta_{slow} = 6.9\text{dB/cm/MHz}$, $v_{fast} = 2100\text{m/s}$, $v_{slow} = 1500\text{m/s}$, [1, 2]. It is these parameter values that we seek to recover in the Bayesian analysis. The other model parameters, γ , l and σ , were systematically varied in the synthesized data to assess the performance of Bayesian methods under various conditions. First, data with signal-to-noise ratios of 500:1, 100:1 and 50:1 were generated. Next, data sets with varying overlaps between the fast and the slow wave were produced by changing the samples thickness l . The overlap was quantified as

$$\text{overlap} [\%] = \frac{t_{pulse} - l(1/v_{slow} - 1/v_{fast})}{t_{pulse}} \times 100\% \quad (14)$$

in which t_{pulse} is the temporal length of the unpropagated pulse. Last, data sets were also generated by varying the relative fraction of fast and slow wave, γ .

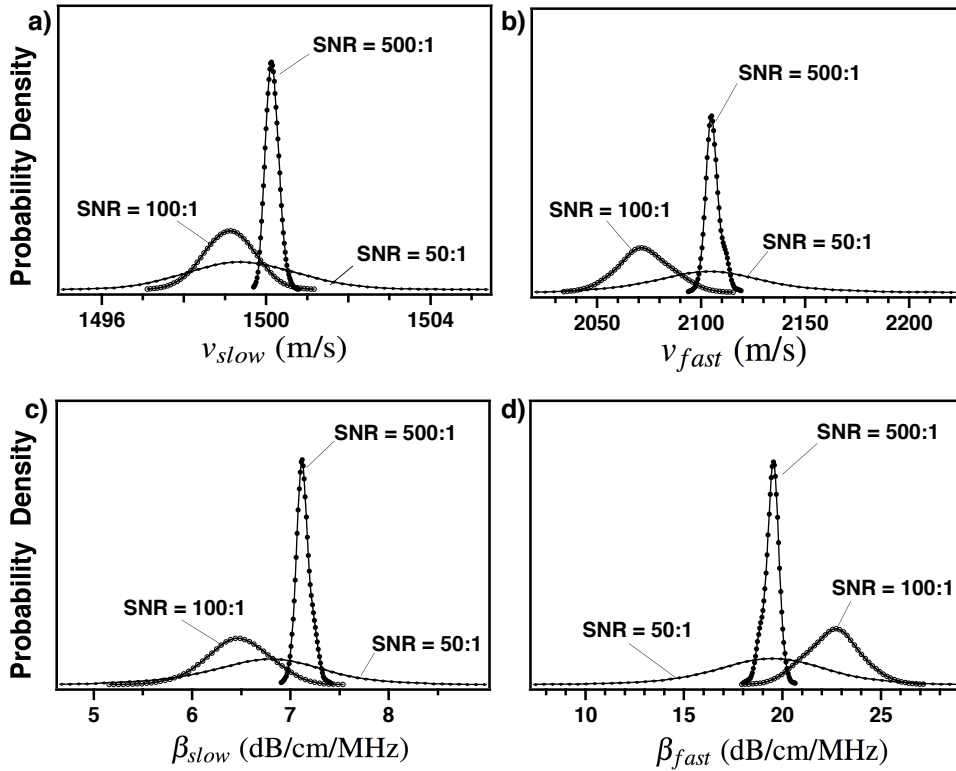


FIGURE 2. The marginal posterior probability density functions for v_{slow} (panel **a**), v_{fast} (panel **b**), β_{slow} (panel **c**) and β_{fast} (panel **d**). Posterior probabilities shown in each plot are computed from simulated data with peak signal-to-noise ratio set at 500:1, 100:1 and 50:1 level.

A plot of some of the marginal posterior probability density functions are given in Fig. 2. These posterior probabilities were computed using three simulated data sets having signal-to-noise ratios of 500:1, 100:1 and 50:1 respectively. As illustrated in Fig. 2, the widths of the posterior probabilities scale inversely with the signal-to-noise ratio. However, close inspection of scales in panels **a** and **b**, reveals that the widths of the posterior for the fast waves parameters are roughly 15 times greater than the posterior probabilities associated with the slow waves parameters. This is in part due to the specific values of parameters used to simulate the data. The analyzed waveform is composed of 70% slow wave and 30% fast wave. The fast wave is highly attenuated. The signal-to-noise ratio is markedly lower for the fast wave than for the slow wave. Consequently, the large widths of the posterior probability density functions for the parameters of the fast wave.

The parameter estimates for all of the simulated data are summarized in Fig. 3. These summaries are mean \pm standard deviation parameter estimates. The mean for a given data set is represented by the dark bar, the standard deviations by error bars and the true value of each parameter are represented by the line. The percents at the bottom of this figure are the percent fast and slow waves in the simulated data. The standard deviations are smallest for the 500:1 signal-to-noise ratio data and increase as the noise

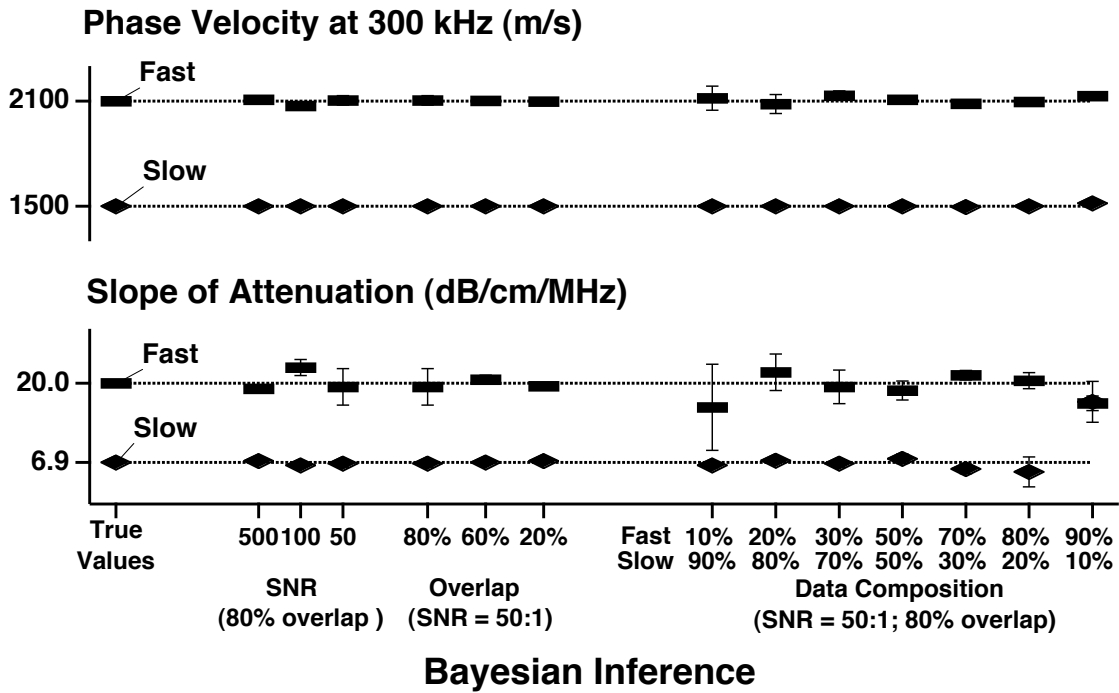


FIGURE 3. The true values for the phase velocity at 300kHz and the slope of attenuation for the fast and the slow wave are compared to the mean \pm standard deviation estimates computed from marginal posterior probability for each parameter. In all cases the Bayesian posterior probabilities overlap the true value used in generating the simulated data.

level increases. Signal-to-noise ratio of 100:1 are typical for data acquired *in vitro*, whereas a lower value is anticipated in measurements *in vivo*. Except for the first three cases, the parameter estimates shown in Fig. 3 are for 50:1 signal-to-noise ratio data. For all the data, the estimated parameter values lie within one or two standard deviations of the true values.

Although the complementary problem of model selection is beyond the scope of this paper, we briefly examine the results of analyzing simulated bimodal data using both a one-mode and a two-mode model, Fig. 4. Panels **a** and **b** are the simulated bimodal data, we have repeated the data in panel **b** for easier comparison. The simulated bimodal data are comprised of 30% fast wave and 70% slow wave with 80% overlap. The peak signal-to-noise ratio of 50:1. Panels **c** and **d** are models generated from the parameters that maximized the joint posterior probability for the parameters when the data are analyzed using a one-mode model (panel **c**) and a two-mode model (panel **d**). The residuals, the difference between the data and the model, are shown in panels **e** and **f**. Panel **e**, the residuals generated from the one-mode model, have a strong systematic artifact; while, panel **f**, the residuals generated from the two-mode model, are random and on the order of the noise. While panels **e** and **f** are suggestive that a two-mode model is needed to explain this data, it is not enough. One needs to go further and compute the posterior probability for the models before one can know for certain, see [7] for more details on

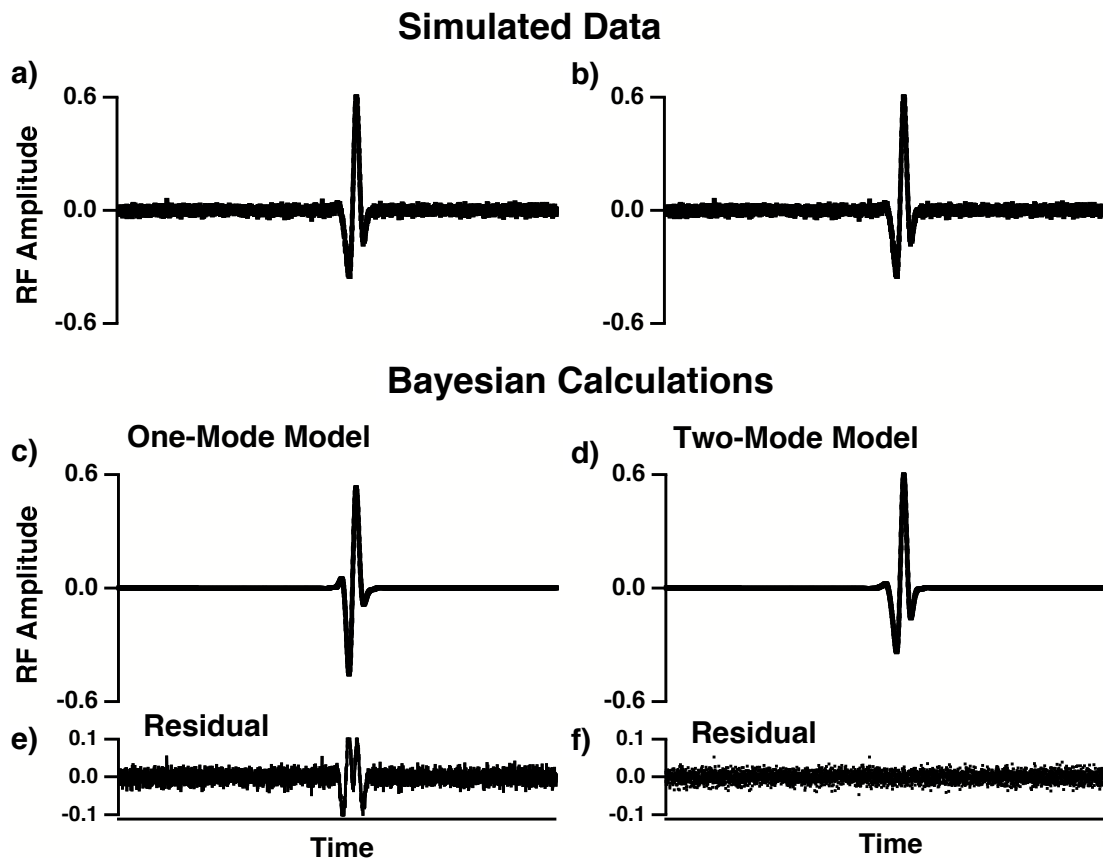


FIGURE 4. A comparison of the residuals generated when bimodal simulated data (panels **a** and **b**) are analyzed using a one-mode and a two-mode model. Panel **c** is the model generated from the parameters that maximized the joint posterior probabilities for the parameters given a one-mode model; while panel **d** is the model generated from the parameters that maximize the joint posterior probability given a two-mode model. The residuals for each model are shown on panels **e** and **f**, respectively. The simulated bimodal data are comprised of 30% fast wave and 70% slow wave with 80% overlap. The peak signal-to-noise ratio is 50:1.

how this is done.

SUMMARY

We have applied the Bayesian probability theory to simulated data containing both a fast and a slow wave that mimic those seen in trabecular bone. Conventional phase and power spectroscopy analyses have no mechanism to handle these bimodal data. However, Bayesian probability theory provides a rigorous approach to analyzing such data. In all of the investigated data sets, including low signal-to-noise ratio data, the Bayesian posterior probabilities cover the true value of the parameters. Thus the Bayesian ap-

proach is an effective method for extracting properties of bone both *in vitro* and *in vivo*.

REFERENCES

1. Waters, K.R. and Hoffmeister, B.K. (2005). Kramers-Kronig analysis of attenuation and dispersion in trabecular bone. *J Acoust Soc Am*, 118(6):3912–3920.
2. Hosokawa, A. and Otani, T. (1998). Acoustic anisotropy in bovine cancellous bone. *J Acoust Soc Am*, 103(5):2718–2722.
3. Padilla, F. and Laugier, P. (2000). Phase and group velocities of fast and slow compressional waves in trabecular bone. *J Acoust Soc Am*, 108(4):1949–1952.
4. Hughes, E.R., Leighton, T.G., Petley, G.W. and White, P.R. (1999). Ultrasonic propagation in cancellous bone: a new stratified model. *Ultrasound Med Biol*, 25(5):811–821.
5. Marutyan, K.R., Holland, M.R. and Miller, J.G. (2006). Anomalous negative dispersion in bone can result from the interference of fast and slow waves. *J Acoust Soc Am*, 120(5):EL55–61.
6. Jeffreys, H. (1961). *Theory of probability*. The International series of monographs on physics. Clarendon Press, Oxford, 3rd edition.
7. Anderson, C.A., Marutyan, K.R., Wear, K.A., Holland, M R amd Miller, J.G. and Bretthorst, G.L. (2007). Model selection in ultrasonic measurements on trabecular bone. Ed. Mohammad-Djafari A, Maximum entropy and Bayesian methods in science and engineering, in this issue.